CEBAF Program Advisory Committee Nine Proposal Cover Sheet

This proposal must be received by close of business on Thursday, December 1, 1994 at:

CEBAF
User Liaison Office, Mail Stop 12 B
12000 Jefferson Avenue
Newport News, VA 23606

Proposal Title

Hard Scattering Amplitude for $\vec{e}p \rightarrow e\vec{p}$ in Medium and Heavy Mass Nuclei

Contact Person

Name: Ronald Gilman
Institution: Rutgers University
Address: P. O. Box 849
City, State ZIP/Country: Piscataway, NJ 088855-0849
Phone: (908) 445-5489 **FAX:** (908) 445-4343
E-Mail → Internet: Gilman@Ruthep.Rutgers.EDU or Gilman@CEBAF.GOV

Experimental Hall: A **Days Requested for Approval:** 55

Hall B proposals only, list any experiments and days for concurrent running:

CEBAF Use Only

Receipt Date: 12/15/94 PR 94-120

By: SP

BEAM REQUIREMENTS LIST

CEBAF Proposal No.: _____ Date: _____
(For CEBAF User Liaison Office use only.)

List all combinations of anticipated targets and beam conditions required to execute the experiment. (This list will form the primary basis for the Radiation Safety Assesment Document (RSAD) calculations that must be performed for each experiment.)

Condition #	Beam Energy (MeV)	Beam Current (μA)	Polarization and Other Special Requirements (e.g., time structure)	Target Material (use multiple rows for complex targets — e.g., w/windows)	Target Material Thickness (mg/cm²)
1	1600	100	45%	C + C	1280 + 43
2	"	"	"	Al + C	720 + 43
3	"	"	"	Fe + C	420 + 43
4	"	"	"	Zr + C	300 + 43
5	"	"	"	Au + C	200 + 43
6	3200	100	45%	C + C	1280 + 43
7	4000	100	45%	C + C	1280 + 43
8	5060	36	80%	C + C	2560 + 86
9	"	"	"	Al + C	1440 + 86
10	"	"	"	Fe + C	840 + 86
11	"	"	"	Zr + C	600 + 86
12	"	"	"	Au + C	400 + 86
13	6000	36	80%	C + C	2560 + 86

The beam energies, E_{Beam}, available are: $E_{Beam} = N \times E_{Linac}$ where N = 1, 2, 3, 4, or 5. For 1995, E_{Linac} = 800 MeV, i.e., available E_{Beam} 800, 1600, 2400, 3200, and 4000 MeV. Starting in 1996, in an evolutionary way (and not necessarily in the order given) the follov additional values of E_{Linac} will become available: E_{Linac} = 400, 500, 600, 700, 900, 1000, 1100, and 1200 MeV. The sequence timing of the available resultant energies, E_{Beam}, will be determined by physics priorities and technical capabilities.

LAB RESOURCES REQUIREMENTS LIST

CEBAF Proposal No.: _____ Date: _____
(For CEBAF User Liaison Office use only)

List below significant resources — both equipment and human — that you are requesting *from CEBAF* in support of mounting and executing the proposed experiment. Do not include items that will be routinely supplied to all running experiments, such as the base equipment for the hall and technical support for routine operation, installation, and maintenance.

Major Installations *(either your equip. or new equip. requested from CEBAF)*

none

New Support Structures: none

Data Acquisition/Reduction

Computing Resources: none

New Software: none

Major Equipment

Magnets: none

Power Supplies: none

Targets: none

Detectors: none

Electronics: none

Computer Hardware: none

Other: none

Other

minor equipment: installation of modified target ladder

HAZARD IDENTIFICATION CHECKLIST

CEBAF Proposal No.: _____ Date: _____
(For CEBAF User Liaison Office use only.)

Check all items for which there is an anticipated need.

Cryogenics
- _____ beamline magnets
- _____ analysis magnets
- _____ target
  - type: _____
  - flow rate: _____
  - capacity: _____

Electrical Equipment
- _____ cryo/electrical devices
- _____ capacitor banks
- _____ high voltage
- _____ exposed equipment

Radioactive/Hazardous Materia
List any radioactive or hazadorou toxic materials planned for use:
_____
_____
_____
_____

Pressure Vessels
- _____ inside diameter
- _____ operating pressure
- _____ window material
- _____ window thickness

Flammable Gas or Liquids
- type: _____
- flow rate: _____
- capacity: _____

Drift Chambers
- type: _____
- flow rate: _____
- capacity: _____

Other Target Materials
- ___ Beryllium (Be)
- ___ Lithium (Li)
- ___ Mercury (Hg)
- ___ Lead (Pb)
- ___ Tungsten (W)
- ___ Uranium (U)
- ___ Other (list below)

Carbon (C), Gold(~~Aluminum(Al), Iron~~ Zirconium (Zr)

Vacuum Vessels
- _____ inside diameter
- _____ operating pressure
- _____ window material
- _____ window thickness

Radioactive Sources
- _____ permanent installation
- _____ temporary use
- type: _____
- strength: _____

Large Mech. Structure/System
- _____ lifting devices
- _____ motion controllers
- _____ scaffolding or
- _____ elevated platforms

Lasers
- type: _____
- wattage: _____
- class: _____

Installation:
- _____ permanent
- _____ temporary

Use:
- _____ calibration
- _____ alignment

Hazardous Materials
- ___ cyanide plating materials
- ___ scintillation oil (from)
- ___ PCBs
- ___ methane
- ___ TMAE
- ___ TEA
- ___ photographic developers
- ___ other (list below)

_____
_____

General:

Experiment Class:

- _x_ Base Equipment
- _x_ Temp. Mod. to Base Equip.
- _____ Permanent Mod. to Base Equipment
- _____ Major New Apparatus

Other: modification consists of modified target ladder

Proposal for the PAC 9 of CEBAF (Jan./Feb. 1995)

Hard Scattering Amplitude for $\vec{e}p \rightarrow e\vec{p}$ in Medium and Heavy Mass Nuclei

R. Gilman [a] (contact person), P. M. Rutt [b] (spokesperson),
E. J. Brash [a] (co-spokesperson), S. Nanda [c] (co-spokesperson)

[a] *Rutgers University, Box 849, Piscataway, NJ 08855.*

[b] *University of Georgia, Athens, GA, 30602.*

[c] *CEBAF, 12000 Jefferson Avenue, Newport News, VA, 23606.*

A Hall A Collaboration Proposal

CEA-Saclay (France), Chungnam National University (Korea)

College of William & Mary, CEBAF, Duke University

IPN Orsay (France), Kharkov Inst. of Physics and Technology (Ukraine)

M.I.T., Norfolk State University, Old Dominion University

Rutgers University, University of Georgia, University of Kentucky

University of New Hampshire, Yerevan Physics Inst. (Armenia)

ABSTRACT

We propose to measure the ratios F_2/F_1 and G_E/G_M in nuclei at low and high Q^2. The results, combined with concurrent high precision relative cross section measurements, will determine for the first time the hard scattering $\vec{e}p \rightarrow e\vec{p}$ scattering amplitude in nuclei. They will permit a high precision determination of possible effects of color transparency with essentially no model dependence. The low Q^2 results will provide a baseline for understanding the high Q^2 results. They will yield a measurement of G_E/G_M in nuclei with small systematic error. These values will be compared with previous values determined by Rosenbluth separation which are decreased by about 25% from free nucleon values.

The ratio of recoil proton polarization components P_t/P_l determines the ratios of form factors, G_E/G_M and F_2/F_1. The cross sections can be used to determine an A-dependent attenuation and an A-independent hard scattering amplitude in nuclei. The absolute magnitude of each form factor is determined from the ratio plus the scattering amplitude.

We propose to measure the $(\vec{e}, e'\vec{p})$ reaction on ^{12}C, ^{27}Al, ^{56}Fe, ^{90}Zr, and ^{197}Au in quasifree kinematics at two values of the four–momentum transfer, Q^2. The first phase of these measurements will determine the ratios G_E/G_M and F_2/F_1 to 10% for each target with 1.6 GeV beam energy at $Q^2 \approx 1$ $(GeV/c)^2$, in about two days of beam time per target. The second phase of these measurements will determine the ratios F_2/F_1 to 10% and G_E/G_M to 14% for the lighter targets with 5.1 GeV beam energy at $Q^2 = 4$ $(GeV/c)^2$, in about one week of beam time per target. Relative cross sections will be determined with a statistical precision much better than 1%, and systematic uncertainties of typically 2 – 3%, for both kinematics. The Q^2 evolution of the form factors will also be measured at additional kinematic points with the lightest target, ^{12}C.

1 Motivation

1.1 Introduction

We propose to use the $(\vec{e}, e'\vec{p})$ reaction to investigate basic properties of protons in moderate and heavy mass nuclei. The physics issues of interest are possible changes in the proton form factors in nuclei (now essentially unknown), proton propagation in nuclei (known with low precision), and the Q^2 dependence of the form factors and proton propagation. We investigate the ratio of proton form factors in the nucleus by measuring polarization transfer. The ratio of the form factors is a fundamental property which can be measured with high precision; it is crucial also in a sensitive search for color transparency. We determine the nuclear attenuation by measuring precise relative cross section data at the same time. Absolute cross section data will then be used with the form factor ratio and nuclear attenuation to determine the absolute magnitudes of the form factors (and thus the elementary effective hard scattering cross section inside the nucleus).

At low Q^2, we expect the form factors and attenuations to be essentially separate issues. This experiment is related to earlier longitudinal / transverse separations in ^{56}Fe(e, e') which found that the Coulomb sum rule still appears quenched at $Q^2 = 1$ (GeV/c)^2, and to longitudinal / transverse separations in $(e, e'p)$ that found a decrease of $\approx$25% in the ratio G_E/G_M for Q^2 about 0.05 to 0.45 (GeV/c)^2. (If one instead describes the proton structure in terms of the Dirac and Pauli form factors, the ratio F_2/F_1 is enhanced $\approx$33%.) At high Q^2, the attenuation issues include the possibility of color transparency (CT). The form factor ratio allows a superior test for this phenomenon, since, as we will discuss, CT effects should be much more noticeable in one

form factor than in the other. This is then a second generation CEBAF CT experiment; it will provide compelling experimental evidence pro or con due to the simultaneous measurement of form factors and attenuation. The separation allows a check on whether it is appropriate to use the free ep amplitude in a nucleus. The only evidence, at low Q^2, suggests that it is not.

1.2 Discussion

The starting points for this investigation include two types of experiments. The first type consists of measurements of proton attenuation in nuclei in $(e, e'p)$. The second type consists of measurements of the proton form factors in nuclei, which have been extracted from longitudinal - transverse separations in $(e, e'p)$ measurements.

An investigation of color transparency (CT) has been carried out by the SLAC NE18 collaboration.[1, 2] The first data reported were cross sections for carbon with uncertainties of 8 - 10% for Q^2 in the range 1 – 7 $(GeV/c)^2$. The proton attenuation was consistent with being constant across this range of Q^2. Thus, it was concluded that no evidence for CT was seen. Since the effects of CT are generally expected[1, 3, 4] to be no more than about 10% for these kinematics, it is difficult to make a definitive conclusion either way. Too, one must consider various nuclear effects and their energy dependence, as will be discussed later.

Cross sections were also measured on Fe and Au targets, with uncertainties of 8 – 22%, for Q^2 in the range 1 – 7 $(GeV/c)^2$. They used the data on all the targets to investigate the A dependence, and to determine an average nuclear attenuation for all targets. Of course, since they assumed that the ep amplitude in a nucleus was unchanged from its free value, the cross section measured on one nucleus determines the attenuation cross section. The use of multiple targets allowed a consistency check, and an improvement in

experimental systematic uncertainties. The attenuation was approximated with a $1/\sigma\rho$ model. In this model they determined that the measured transmissions are consistent with a ≈30 mb absorption cross section, as compared to the free pp and pn cross sections, which are each ≈40 mb.

This overall difference is not surprising, even apart from uncertainty in the actual value of the elementary *ep* cross section inside nuclei. Previous transmission measurements[5, 6] at $Q^2 \approx 0.3$ $(GeV/c)^2$ showed an enhancement of a factor of two over simple expectations, apparently resulting[7] from nuclear effects including Pauli blocking, correlation holes, and the velocity dependence of the interaction. The effective attenuation cross section was about 12 mb, as compared to the free cross section of about 25 mb. This shows how important it is in such studies to have a true signature of color transparency, and not just transparency alone.

Investigations of the nucleon form factors in nuclei[8, 9, 10, 11] have used Rosenbluth separations to determine that the ratio G_E/G_M is decreased by about 25%, for Q^2 between about 0.05 and 0.45 $(GeV/c)^2$. The data – see Fig. 1 – are limited, but there is no evidence for any dependence on any parameter. What to make of these data is unclear. As has been discussed previously,[12] questions exist about reaction mechanism corrections to the data – the form factor ratio is model dependent, and may be explained by rescattering and other effects.[13, 14, 15] Too, there exist estimates that, in the nuclear medium, changes in the nucleon form factors should[16, 17, 18, 19, 20] and should not[21] be expected. If one accepts these data as evidence of modifications to the proton form factor in nuclei, then it becomes unjustified to use the free *ep* amplitude for *ep* scattering in a nucleus. It is necessary to determine both the nuclear attenuation and the in-medium scattering amplitude from the data itself.[22] This is one of the goals of the current experiment, and justifies our plan to simultaneously measure cross sections and polarizations.

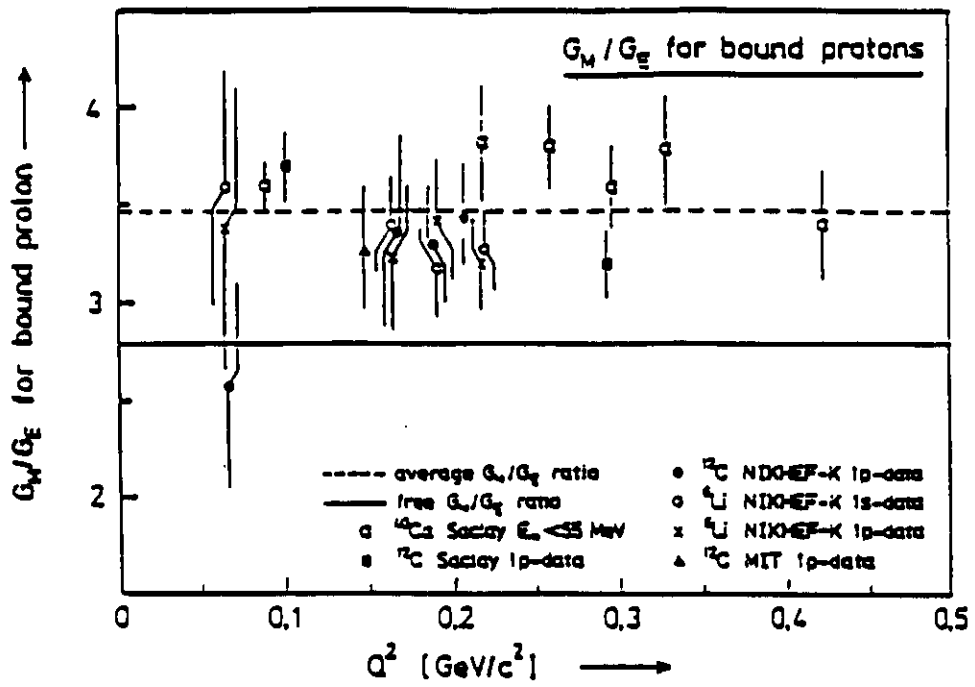

Figure 1: The ratio G_M/G_E extracted from $(e, e'p)$ experiments. This is the inverse of the ratio as discussed in the text.

1.3 Color Transparency and the F_2 Form Factor

Our experimental goals include both a study of the ep scattering amplitude in nuclei and the subsequent proton propagation through these nuclei. Experimentally, these issues cannot be simply factorized and independently investigated. Indeed, it has recently been suggested[23] that color transparency will itself modify the observed nucleon form factors in nuclei. The argument is as follows.

Helicity conservation is an approximate symmetry of quantum chromodynamics (QCD), and should become exact in the limit $m/E \to 0$. Since the masses of the quarks are small, it is more generally expected to hold at the quark level than at the nucleon level. The proton structure may be described

in terms of two form factors, the helicity conserving Dirac form factor, F_1, and the helicity nonconserving Pauli form factor, F_2 – these are related to the usual Sachs electric and magnetic form factors, as shown in Section 2.1. If F_2 resulted from helicity flips of the quarks in the nucleon, it should be very small compared to F_1. A simple estimate[24] is that F_2 should be suppressed relative to F_1 by factors of m^2/Q^2, where m is an effective quark mass, plus some unknown overall relative normalization, which we will assume to be unity. With an effective quark mass m about the current quark mass, a few MeV, we expect $Q^2F_2/F_1 = m^2 \approx 10^{-5}$. Using a constituent quark mass, the estimate is nearer 10^{-1}. Experimentally it has been found[25] that the ratio Q^2F_2/F_1 is consistent with being constant and approximately unity for Q^2 above about 2.5 – 3 $(GeV/c)^2$. It appears [1] that F_2 is large relative to F_1, and thus F_2 probably does not arise from helicity flips at the quark level.

It is known from deep inelastic scattering that the spin of the valence quarks constitutes only about 30% of the angular momentum of the nucleon – the remainder is carried by gluons, sea quarks, and orbital angular momenta. This makes plausible a suggestion[28, 29] that the proton F_2 form factor results from relative orbital angular momentum between quarks in the proton rather than from a quark helicity flip. The point is that one can add angular momenta of $\vec{1}$ and $\frac{\vec{1}}{2}$ to get $\frac{\vec{1}}{2}$, pointed in the opposite direction. Thus, hadron helicity is not conserved.

Let us now consider hard scattering of an electron from the proton. A useful physical picture is that, as Q^2 increases, the virtual photon samples smaller fractions of the spatial extent of the proton. Elastic scattering will occur only when the proton valence quarks are spatially closer together at higher Q^2. For scattering proceeding via the F_1 form factor, the valence quarks may have 0 transverse separation, leading to a small proton. For

[1] The 200 – 300 MeV quark mass used in diquark / constituent quark models[26, 27] allows larger helicity violations, so that these models can reproduce the size of the F_2 form factor. The correctness of the explanation is open to question.

scattering proceeding via the F_2 form factor, however, the requirement of an orbital angular momentum forces a transverse separation of the quarks. Since $\vec{L} = \vec{r} \times \vec{p}$, r cannot go to 0. In effect, the "F_2" proton has a larger transverse size than the "F_1" proton.

This difference has implications for hard scattering in a nucleus. The simplest estimate one can make, based on this argument, is that one expects a color transparency effect for F_1, but not for F_2. That is, for hard *ep* scattering in a nucleus in kinematics for which there is some CT effect, the "large F_2 proton" is expected to be more attenuated by the required subsequent proton propagation through the nucleus than is the "small F_1 proton". The apparent ratio one observes for F_2/F_1 is reduced from that characteristic of the hard *ep* scattering process in the nucleus. It is this change in the apparent ratio, a change which is accentuated as A increases, which we will use as a signature of possible color transparency. [Of course, correction for the difference in attenuation in the two channels would recover the true ratio of F_2/F_1 in the nucleus.] Thus CT would result in an apparent enhancement to the ratio G_E/G_M, since G_E results from a difference between F_1 and F_2, whereas G_M results from a sum.

A simple numerical estimate of some possible effects on the polarizations we measure, and the resulting apparent form factor ratios, is given in Table CT.1 for a ^{12}C target in the $Q^2 = 4$ (GeV/c)^2 kinematics. The column labelled "free" gives predictions using a free form factor and the same attenuation for F_1 and F_2. The column labelled "FF" uses modified form factors in the nucleus, estimated from [20]. The column labelled "CT" uses the free form factors, but with different attenuation cross sections - 30 mb for F_2 as suggested by NE18 data, but 15 mb for F_1 as suggested by color transparency analyses. For ^{12}C data, we expect to obtain about 3 – 4% uncertainties on the form factor ratios, due to the extra statistics obtained with the normalization target. Effects of the magnitudes suggested below will be observable.

The sizes of both the effects and the experimental uncertainties increase for larger targets.

Table CT.1 :

Estimate of some possible effects for this experiment.

Effect	FF	(free)	CT
Apparent Q^2F_2/F_1	1.14	0.96	0.88
Apparent G_E/G_M	0.28	0.36	0.40
P_t/P_l	-.24	-.31	-.35
P_t	-.15	-.19	-.20
P_l	0.61	0.59	0.58

1.4 Unique Features

Some important features of this experiment, and differences from previous proposals, include the following:

1. Polarization transfer data will determine the form factor ratios G_E/G_M and F_2/F_1 to typically 10–15%. These ratios will be determined at low missing momentum, a region in which they are expected to be insensitive to rescattering of the outgoing nucleon. We believe that one *must* investigate polarization transfer to investigate more precisely whether the free and in-medium *ep* amplitudes differ.

2. Experimentally, we determine the polarization transfers using both signs of the electron helicity, thus removing false asymmetries associated with the polarimeter. Taking the ratio of polarization components approximately removes all systematic uncertainties associated with polarimeter analyzing power and the beam polarization. The largest remaining systematic uncertainty, spin transport through the spectrometer, is small compared to statistical uncertainties.

3. Polarization transfer measurements require large numbers of counts, allowing a concurrent determination of cross sections to the 0.1% level statistically. Thus, cross section uncertainties are dominated by systematic uncertainties.

4. To ensure very precise relative cross sections, for determination of the proton attenuation, we will use a double target consisting of the nuclear target of interest plus a thin normalization carbon foil located upstream of the target. The foil will give better than 1% relative normalizations, checking the product of spectrometer efficiencies and integrated beam current. The largest remaining systematic uncertainties will be theoretical corrections related to the limited phase space in missing momentum and energy covered by the Hall A spectrometer system. The resulting cross section precisions should be about five times better than those of NE18.[2]

5. While precise polarization measurements require an integration over missing momentum and missing energy, equivalent to the Fermi momentum and the orbital of the struck particle within the plane wave impulse approximation, precise ($\approx$ 1%) relative cross sections can be determined for small bins in missing momentum and missing energy. This results from the $\approx 10^6$ counts needed for the polarization determination, plus the high precision of the Hall A spectrometers. Thus, attenuation can be investigated as a function of orbital and Fermi momentum.

6. Except for measurements on ^{16}O at $Q^2 = 1$ (GeV/c)^2, all existing polarization transfer proposals are on light nuclei. We believe it is important to do this measurement on medium and heavy nuclei, to reduce any possible A dependence effects other than attenuation, and to be able to study binding energy and density dependent effects.

7. The $Q^2 = 1$ $(GeV/c)^2$ data will provide a baseline measurement for which no color transparency effects are expected, and for which nuclear effects such as meson exchange currents, isobar configurations, and multinucleon currents are expected to be small. High count rates will allow us to check the dependence of the observed polarizations on Fermi momentum, nucleus, and nuclear orbital.

8. We also propose to measure the Q^2 evolution of the form factors on a single target, ^{12}C. Since the NN cross sections are roughly constant for proton energies corresponding to Q^2 above 1.5 $(GeV/c)^2$, these data should, if there is no CT effect, reveal any Q^2 dependence to the form factors in nuclei.

1.5 Five Targets

We have proposed to measure five targets as part of this experiment, as a result of the following consideration. In any simple analytic A dependence analysis, one has to consider four parameters: renormalization factors and attenuation cross sections for each of the amplitudes F_1 and F_2. It is desirable to have more than four targets to determine these four parameters. The errors in the determination of the four parameters can be estimated simply as follows.

Assuming that one does not have a theoretical model for either the ep amplitude in nuclei or for the recoil proton attenuation, then one can fit the A dependence of the cross sections to determine both quantities. The simplest model uses

$$\sigma(A) = Z\sigma_{ep} f_{atten}(A), \tag{1}$$

where $\sigma(A)$ is the measured cross section, Z is the number of protons, σ_{ep} is the ep cross section in a nucleus, extrapolated to $A = 1$ and assumed to

be independent of nucleus, and $f_{atten}(A)$ is the fraction of protons remaining after attenuation. The simplest estimate for this attenuation uses spheres of radius $R \approx 1.2A^{1/3}$ fm and a constant density of $\rho \approx 0.17$ nucleons / fm^3, plus a $\lambda = 1/\sigma\rho$ attenuation length. The integration can be performed analytically to give[22]

$$f_{atten}(A) = \frac{3}{8}x^3(e^{2x} - 1) + \frac{3}{4}x^2e^{2x} + \frac{3}{4}x \qquad (2)$$

where $x = \lambda/R$. Use of more realistic nuclear densities is certainly possible, and has been done for the NE18 analysis.[2] This simple model can also be extended to include the form factor ratio data.

If either the *ep* cross section or the attenuation is taken to be some known quantity, then the other can be reasonably well determined from existing data. If one assumes the free *ep* cross section, the attenuation cross section is determined to about 10 – 15% for the NE18 data.[2] If both parameters are fit, then correlations between the two increase the uncertainties greatly and the existing data yield large errors. We have refit the NE18 data with the simple model described above, and find typical uncertainties to be about 20% for the *ep* cross section in a nucleus and about 50% for the recoil proton attenuation cross section. In fact, most of the data favor both an enhanced *ep* cross section in nuclei and an attenuation cross section greater than the free *ep* cross section, demonstrating both the correlations between these parameters, and the fact that this simple model does not give a physically acceptable result with these data.

We expect to achieve relative cross section uncertainties of about 3%, with the uncertainty dominated by theoretical corrections. Pseudo-data with these uncertainties were fit. The resulting uncertainties on the derived parameters were:

1. Fixing σ_{ep}, $\sigma_{attenuation}$ was determined to 1.6%.

2. Fixing $\sigma_{attenuation}$, σ_{ep} was determined to 0.7%.

3. Allowing both to vary, σ_{ep} was determined to 5.1%, and $\sigma_{attenuation}$ was determined to 12.6%.

4. Reducing the number of targets, N_{tgt}, to 3, as in NE18, the uncertainties were observed to scale roughly as $1/\sqrt{N_{tgt}}$.

The error on the *ep* cross section can be reduced once the corrections for attenuation have been made for each of the target nuclei. The uncertainty in σ_{ep} cited above is large, since physically it is the uncertainty in the cross section extrapolated to $A = 1$. The fit in the region of the data does not change much if one increases both σ_{ep} and the attenuation, or decreases both. This correlation increases the uncertainty in σ_{ep}. The *ep* cross section in any of the individual nuclei measured is known better than σ_{ep} as determined by the fit, since the variations in $\sigma(A)$ are much smaller in the region of the data than at $A = 1$. One can instead determine the *ep* cross section in a nucleus by correcting each nuclear cross section for the attenuation, then averaging the corrected cross section. This procedure yields the same value for the *ep* cross section, but with uncertainties about three times better than those for the parameter σ_{ep}, since the effect of the correlations in the extrapolation has been removed.

1.6 Relation to Other Experiments

This experiment is complementary to a number of approved CEBAF experiments. In general, it is distinct in that we tie together, and are able to investigate, the issues of polarization transfer to study nucleon form factors in the nucleus and A dependence measurements to study proton propagation through the nucleus.

The structure of the free proton is studied through polarization transfer with recoil proton polarization measurements in exp. 93-027 (C. F. Perdrisat,

V. Punjabi, and M. K. Jones, spokespeople). Studies of the proton form factors in nuclei are approved for the deuteron in exp. 89-028 (J. M. Finn and P. E. Ulmer, spokespeople), ^{4}He in exp. 93-049 (J. F. J. van den Brand, Rolf Ent, and P. E. Ulmer, spokespeople), and ^{16}O in exp. 89-033 (C. Glashausser, C. C. Chang, S. Nanda, and J. W. van Orden, spokespeople). Too, a related proposal[30] to this PAC studies polarization transfer on ^{3}He. The ^{16}O experiment is the only other study not on a few body system. A large fraction of the interest in these approved experiments is the behavior of the recoil polarization for large missing momenta, a region in which there is significant sensitivity to the model of the reaction mechanism. In the current experiment, our interest is in avoiding this region. The ^{4}He experiment will also take data at similar Q^2, which can be considered in an analysis of A dependence in this experiment.

Proton propagation through the nucleus is investigated by cross section measurements in Hall C exp. 91-007 (R. Milner, spokesperson), and 91-013 (D. F. Geesaman, spokesperson). Induced recoil proton polarization, which results from rescattering of the outgoing proton, is studied in Hall A exp. 91-006 (A. Saha, spokesperson). Experiment 91-013 will obtain some longitudinal – transverse separation data for $Q^2 \approx 1$ and 2 $(\mathrm{GeV/c})^2$; a comparison with our data obtained by polarization transfer will be an interesting check on the experimental techniques.

1.7 Summary

We propose to measure high precision polarization transfer ratios and cross sections for reactions $A(\vec{e}, e'\vec{p})$. Our interests are the proton form factor in nuclei and the rescattering of the struck proton, including the phenomenon of color transparency at high Q^2. We believe these issues cannot be separated, and both must be investigated concurrently, as in this experiment, if one is to understand these issues.

A measurement of the A dependence at $Q^2 = 1$ (GeV/c)^2 provides an excellent measurement of the form factors and nuclear transparency. Meson exchange currents, related nuclear effects, and color transparency effects should be small or nonexistent in these kinematics. These high precision data will test the polarization transfer technique. The proton nucleus interaction has been extensively studied at this energy, and extensive related $^{16}O(e,e'p)$ measurements are planned, both with and without polarization. A Q^2 dependence on ^{12}C will then be used to investigate any energy / Q^2 dependence of the form factors on ^{12}C. Finally, an A dependence measurement at $Q^2 = 4$ (GeV/c)^2 will allow additional testing of the form factors and proton rescattering effects in kinematics where color transparency effects may be detectable.

2 Background

In the following sections, we discuss in more detail the physics background for this experiment. The discussion is divided into three sections, a discussion on electron scattering from the free proton, a discussion of how the amplitude is different for a bound proton, and a discussion of the propagation of the struck proton through the nucleus.

2.1 Electron Scattering from the Free Proton

In elastic e-p scattering, the energies of the incident (E_e) and scattered (E'_e) electrons and the kinetic energy of the scattered proton (T_p) are related to the four-momentum transfer Q^2 by:

$$Q^2 = 2\,M_p\,T_p = 2\,M_p\,\omega = 2\,M_p\,(E_e - E'_e) \approx 4E_eE'_e\sin^2\left(\frac{\theta_e}{2}\right) \qquad (3)$$

where M_p is the proton mass and θ_e the scattering angle of the electron.

The differential cross section can be written[31, 32] as

$$\frac{d\sigma}{d\Omega} = \left(\frac{d\sigma}{d\Omega}\right)_{NS} \cdot \left(\frac{G_E^2 + \tau G_M^2}{1+\tau} + 2\tau G_M^2 \tan^2(\theta_e/2)\right), \tag{4}$$

or alternatively as

$$\frac{d\sigma}{d\Omega} = \left(\frac{d\sigma}{d\Omega}\right)_{NS} \cdot \left(F_1^2 + \tau\kappa^2 F_2^2 + 2\tau(F_1 + \kappa F_2)^2 \tan^2(\theta_e/2)\right), \tag{5}$$

where

$$\left(\frac{d\sigma}{d\Omega}\right)_{NS} = \frac{E_e'}{E_e} \cdot \frac{\alpha^2 \cos^2 \frac{\theta_e}{2}}{4E_e^2 \sin^4 \frac{\theta_e}{2}} \tag{6}$$

describes the scattering of an electron off a pointlike spinless particle (α is the fine structure constant),

$$\kappa_p = \mu_p - 1 = 2.79 - 1 = 1.79, \tag{7}$$

$$\tau = Q^2/4M_p^2, \tag{8}$$

and G_E is the Sachs electric form factor, G_M is the Sachs magnetic form factor, F_1 is the helicity conserving Dirac form factor, and F_2 is the helicity nonconserving Pauli form factor. The electric and magnetic form factors can be related to the Pauli and Dirac form factors, assuming current conservation and a free nucleon, as

$$G_E = F_1 - \tau\kappa_p F_2, \tag{9}$$

$$G_M = F_1 + \kappa_p F_2, \tag{10}$$

$$F_1 = \frac{G_E + \tau G_M}{1+\tau}, \tag{11}$$

and

$$F_2 = \frac{G_M - G_E}{\kappa_p(1+\tau)}. \tag{12}$$

The proton form factors can also be approximately characterized in terms of the "dipole" form factor, G_D, as follows:

$$G_D = \left(\frac{1}{1 + Q^2/0.71(GeV/c)^2}\right)^2, \tag{13}$$

$$\frac{G_M}{\mu_p} = G_E = G_D, \tag{14}$$

$$\frac{F_1}{1 + \mu\tau} = F_2 = \frac{1}{1 + \tau} \cdot G_D. \tag{15}$$

Note that these transformations given above do *not* mean that F_2 is exactly the size one should expect, and consistent with quark helicity flip. $G_E(Q^2 = 0) = 1$ is required by the charges of the quarks in the proton, but $G_M(Q^2 = 0) = \mu_p$ results from those charges and the wave function of the nucleon. The size of F_2 depends on the scattering mechanism and the nucleon wave function, and the details of this process could have led to a physically smaller F_2 and a value of μ_p near 1, or a physically larger F_2 and a value of μ_p very much larger than 2.79. These transformations do not of themselves imply that F_2 is either large or small relative to F_1 (compared to what one expects from quark helicity flip).

The recoil proton has no polarization if the electron beam is unpolarized. The longitudinal (in the $\vec{q}$ direction) component P_l and the transverse (in scattering plane) component P_t are zero due to parity invariance. The normal component (perpendicular to the scattering plane) P_n is zero for the proton or for a nuclear target, in the plane-wave impulse approximation. However one expects P_n to be generally nonzero on a nuclear target.

The polarization transfer components for the proton can be written[34, 33, 35] most simply in terms of the electric and magnetic form factors as follows:

$$I_0 P_t = -2h\sqrt{\tau(\tau + 1)} G_E G_M \tan(\theta/2), \tag{16}$$

and

$$I_0 P_l = h\frac{E_e + E'_e}{M}\sqrt{\tau(\tau + 1)} G_M^2 \tan^2(\theta/2), \tag{17}$$

where I_0 is the combination of form factors from the cross section expression above, and h is the beam helicity. In fact, each of the polarizations actually depends only the the ratio of form factors, as can be seen by carrying out the divisions indicated above. Using $R_G = G_E/G_M$, we can rewrite I_0 as:

$$I_0 = G_M^2\Big(\frac{R_G^2+\tau}{1+\tau} + 2\tau\tan^2(\theta/2)\Big). \tag{18}$$

Carrying out the divisions, we obtain:

$$P_t = \frac{-2h\sqrt{\tau(\tau+1)}R_G\tan(\theta/2)}{\frac{R_G^2+\tau}{1+\tau} + 2\tau\tan^2(\theta/2)} \tag{19}$$

and

$$P_l = \frac{h\frac{E_e+E'_e}{M}\sqrt{\tau(\tau+1)}\tan^2(\theta/2)}{\frac{R_G^2+\tau}{1+\tau} + 2\tau\tan^2(\theta/2)}. \tag{20}$$

While each polarization transfer depends only on the ratio of form factors, using these expressions to determine the form factor ratio allows significant systematic uncertainties related to knowledge of absolute beam polarization and analyzing power of the proton polarimeter. *One can instead take the ratio of polarization components, so that these systematic uncertainties cancel.* After rearranging, one finds:

$$R_G = \frac{P_t}{P_l}\cdot\frac{(E_e+E'_e)\sin(\chi)\tan(\theta/2)}{-2M_p}. \tag{21}$$

Here, the added factor of $\sin(\chi)$ explicitly gives the first order spin precession effects on P_l as the protons pass through the magnetic spectrometer. Essentially all systematic uncertainties cancel in the expression above. The ratio of form factors does not depend on beam helicity or polarimeter analyzing power - although these quantities will affect the uncertainty on the ratio. The kinematic and spin precession factors are known quite precisely – as shown in Section 3.4. Thus, the relative uncertainty in the form factor

ratio is essentially equal to the relative uncertainty in the polarization components. The equations presented above, converted to neutron parameters, also provide the basis for the measurement of the neutron electric form factor through recoil polarization in CEBAF exp. 93-038 (R. Madey, spokesperson).

The ratio of Pauli to Dirac form factors can be written as

$$R_F = \frac{F_2}{F_1} = \frac{1 - G_E/G_M}{\kappa(\tau + G_E/G_M)} \tag{22}$$

The relative uncertainty on this ratio is of similar size to that on the ratio of electric to magnetic form factors - see Section 3.4.

The form factors discussed above have been extracted over varying ranges of Q^2. Because of the kinematic enhancement of the magnetic over the electric form factor by a factor of τ, the cross section becomes nearly all magnetic for four momentum transfers above several $(GeV/c)^2$. The magnetic form factor has been extracted[36, 37] to $Q^2 = 31$ $(GeV/c)^2$, but the electric form factor has been extracted[25] only to several $(GeV/c)^2$, and with perhaps 20% systematic uncertainties. The same kinematic factor enhances F_2 relative to F_1, but since F_2 falls off as asymptotically Q^{-6} instead of Q^{-4}, the relative contribution of these two form factors to the cross section is more nearly constant than in the case of magnetic and electric form factors. The Dirac and Pauli form factors have been extracted over the same range as the electric form factor.

2.2 Electron Scattering from a Bound Proton

In the discussion above, we have suggested two possible differences between scattering of an electron from a free proton and from a bound proton, that the individual form factors and the overall cross section might change. There are a number of aspects to this problem; we might consider these to approximately divide into two categories, changes to the structure of the pro-

ton in the nucleus, and additional amplitudes explicitly involving multiple nucleons. In this section, we will consider some possible mechanisms that affect the scattering vertex.

One might expect in general that there should be a change in the scattering amplitude, since the binding of the nucleon in the nucleus changes its mass, and thus its wave function. Estimates have been made in both quark[17, 20, 38] and relativistic nuclear[16, 18] models. These calculations indicate large effects are possible, but the calculations are certainly not definitive.

Since the electron scatters from a proton in the nucleus, it is formally incorrect to use the on-shell form factors for the free proton; one should instead use the 6 half-off-shell form factors to describe the process. These form factors are not as well understood theoretically as the free form factors, but have been investigated in some physical models. (Experimental analyses commonly uses off-shell extrapolations[39] with the on-shell form factors.) Some recent work[40, 41] has estimated the off-shell form factor corrections using one pion and one kaon loops. For (e, e') reactions, the main effect of the off-shell form factors is a reduction of perhaps 20% in both the longitudinal and transverse responses near $q = 0.5$ GeV/c. The reduction factor is about A independent for the calculated nuclei. We show in Fig. 2 data and calculations[41] for longitudinal and transverse response functions in ^{12}C and ^{238}U. Comparison between calculations and data for each response function in the two nuclei are similar. The calculations reproduce the factor of $\approx$15 increase in strength from ^{12}C to ^{238}U, which agrees with ratio of protons for the two nuclei. While one expects about two-thirds of the nucleons to be within 1 fm of the surface of ^{12}C, but only one-third of the nucleons to be within 1 fm of the surface of ^{238}U, the ratio of transverse to longitudinal strengths is the same in the two nuclei. This ratio is roughly 1.5 in the calculations, and 2 in the data, for each nucleus.

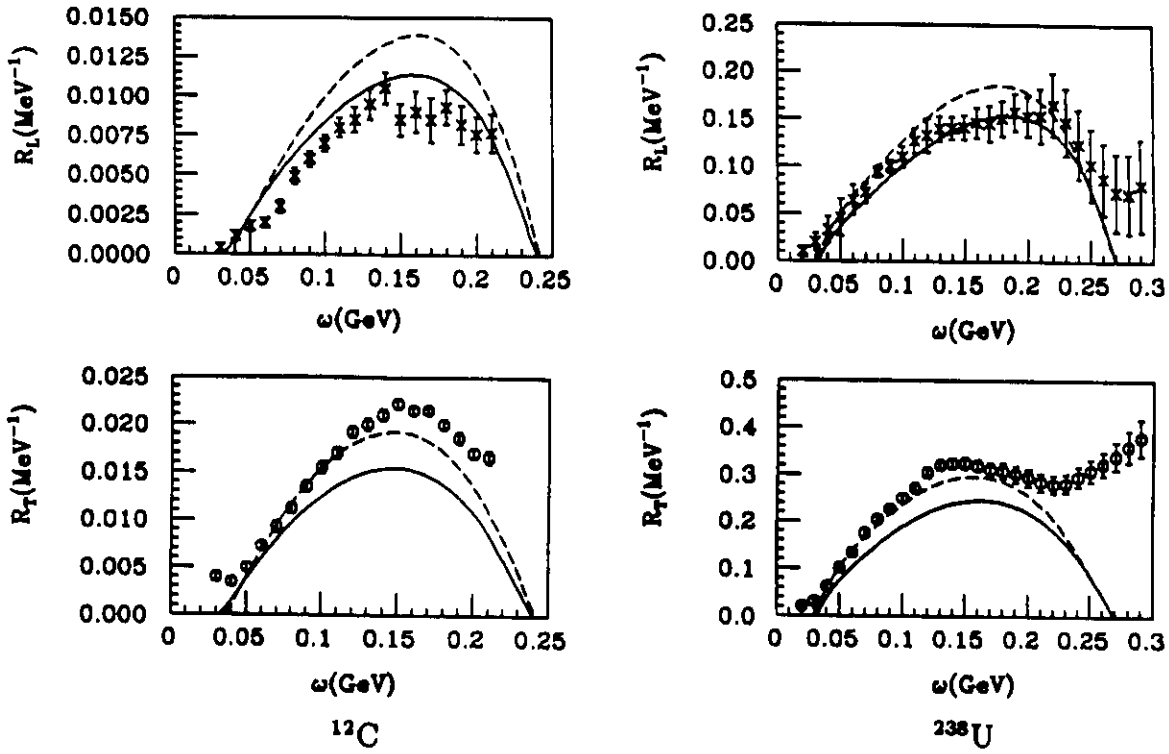

Figure 2: Longitudinal and transverse response functions in ^{12}C and ^{238}U, from [41]. The dotted curves use on-shell form factors; the solid curves use off-shell form factors. Longitudinal and transverse response functions in ^{12}C and ^{238}U, from [41]. The dotted curves use on-shell form factors; the solid curves use off-shell form factors.

Intuitively, one might expect effects to be dependent on the binding energy of the proton, and on the local density of the nucleus near the proton. This might lead to differences for different orbits in a nucleus, and to a gradual A dependence from the decreasing fraction of surface nucleons. Since no orbital dependence was seen in the G_E/G_M ratio extracted from the $(e, e'p)$ data, and no A dependence was seen in the calculations mentioned above, any such dependences would appear to be very weak. If this is the case, one expects the polarization transfer ratio P_l/P_t and the *ep* cross section to also be A independent, and characteristic of an in-medium, rather than free, scattering amplitude, at least for the medium and heavy mass nuclei of this

experiment. This is important since any A dependence could be absorbed into an attenuation cross section, yielding misleading results. Too, this argues against the use of very light nuclei, for which A dependence effects could be much larger. In the (e, e') reaction, the cross section per nucleon is roughly consistent with no A dependence – this is related to the missing strength in the Coulomb sum rule being similar for all these medium and heavy nuclei at the same, lower Q^2, less than about 1 $(GeV/c)^2$. For the He isotopes, the sum rule appears to generally be missing less strength for the same momentum transfer.

Meson exchange currents (MEC), and closely related two-nucleon currents and isobar configurations, are also expected to have effects, especially at smaller Q^2. Schiavella[42] has suggested that the enhancement of magnetic to electric form factors at low Q^2 is consistent with what one expects from meson-exchange / two-body currents. We expect that the importance of MEC should decrease with increasing Q^2, due to a faster falloff by at least a factor[43] of Q^4, from the πNN and $\gamma\pi\pi$ vertices, plus the pion propagator, as opposed to the single γNN vertex. If MEC lead to a 20% effect at Q^2 near 0.25 $(GeV/c)^2$, the effect should be no more than a few percent by Q^2 = 1 $(GeV/c)^2$. This size effect would be difficult to observe. Too, MEC and isobar configurations make little difference in calculated $(\vec{e}, e'\vec{p})$ polarization transfer observables at low missing momentum, as shown for the deuteron by Arenhovel[44] and for ^{3,4}He by Laget[30, 45] at low Q^2.

2.3 Proton Propagation through the Nucleus

2.3.1 Low Energy Proton Propagation

Proton propagation in nuclei is an important consideration in all $(e, e'p)$ reactions. It has been directly studied[5, 6] through the ratio of integrated cross sections for A$(e, e'p)$ to the cross section for A(e, e'). The main observation of this experiment[5, 6] was that for protons with kinetic energies of

about 100 to 180 MeV, the apparent attenuation corresponded to a mean free path in nuclei of about 5 fm, as opposed to the 2.4 fm one might expect from a $1/\sigma\rho$ approximation. It is apparent that nuclear effects such as Pauli blocking and correlations exist that can modify the attenuation from what one expects in a naive approach. These effects have been included in a theoretical explanation[7] of the data by Pandharipandhe and Pieper (PP); distorted wave calculations[46] also approximately reproduce the data. It is possible that the interesting theoretical elements in the PP calculation are effectively included in the distorted wave calculation through the use of an effective interaction that fits nucleon nucleus scattering.

We have made a quick estimate of the size of the Pauli blocking effect by using pp cross sections calculated from the phase shifts of Arndt and collaborators.[47] We integrated the angular distributions to find what fraction corresponded to a recoil proton with momentum less than 300 MeV/c, and considered that fraction to be Pauli blocked. The Pauli blocking estimate was 40% at 150 MeV, 18% at 500 MeV, 14% at 1000 MeV, 12% at 1500 MeV, and 10% at 2000 MeV. In terms of four momentum transfer in $(e, e'p)$ reactions, these energies correspond to $Q^2 \approx 0.3$, 1, 2, 3, and 4 $(\mathrm{GeV/c})^2$. Thus, Pauli blocking should be a smaller effect in the current experiment than in the lower energy data, and should not be a strong function of energy at higher energies.

A second element is the correlation hole. If one views nucleons as point particles, then the short range repulsion leads to a hole in the nuclear density near any nucleon. If one were to plot the density of the nucleus in the rest frame of a particular nucleon, there would be a correlation hole of radius about 1 fm, surrounded by a constant density of about 0.17 nucleons / fm^3, decreasing slowly to 0 as one reaches the nuclear surface. Thus, a struck nucleon can propagate freely some distance before it can interact. Of course, the finite sizes of nucleons will to some extent fill in the correlation hole and

decrease this effect. In PP, the correlation hole leads to a $\approx$ 20% increase of the nuclear transparency. The correlation hole in effect increases transparency by making all nuclei a little smaller. The low Q^2 points will test these ideas with better precision than existing data.

2.3.2 High Energy Proton Propagation

It is well known that color transparency (CT) predicts a reduction at large momentum transfer of the strong interactions of a hadron traversing nuclear media. The original arguments for the existence of CT were developed in the context of perturbative QCD [48]. This effect can also be produced in models based on non-perturbative QCD processes. [49] At present there are only two experiments which have attempted to see CT effects, by measuring changes in the absorption of hadrons as a function of the momentum transfer to the struck nucleon (Q^2).

The first experiment, by Carrol et al[50] at Brookhaven National Laboratory, simultaneously measured rates from A(p,2p) and H(p,2p) reactions. This experiment showed evidence of CT at values of $Q^2 \sim 3 - 8$ (GeV/c)^2, but the transparency decreased at higher values of $Q^2 \sim 8 - 11$ (GeV/c)^2. While Ralston and Pire [51] have explained this effect in terms of a process which interferes with the free nucleon-nucleon amplitude, but which is suppressed in the nuclear media, there is ambiguity as to how these results should be interpreted in terms of CT. The other experiment was discussed in the Motivation, Section 1.2; it was performed at SLAC by the NE18 collaboration via the A$(e, e'p)$ reaction on D, C, Fe, and Au targets.[1, 2] This experiment found no significant rise in CT for any of the nuclei studied over a Q^2 range of $\sim 1 - 7$ (GeV/c)^2. The present experiment measures cross sections with precision improved to a factor of about five better than NE18, in addition to measuring the form factor ratio.

3 Experimental Details

Our experimental measurements include both polarization transfer and cross sections. Polarization transfer has been described in Section 2.1 above. To measure cross sections, we will run with a proton spectrometer trigger that requires particles to pass only through the front pair of scintillators; the rear scintillator will also be read out. Front wire chamber, Cerenkov detector, and polarimeter information are also available. By not requiring the rear scintillator, which is equivalent to putting the polarimeter in the trigger, we can obtain absolute cross sections while retaining all good polarimeter events at the expense of a slightly higher data rate. This setup is possible because the experiment is not rate limited.

The targets proposed for this experiment, ^{12}C, ^{27}Al, ^{56}Fe, ^{90}Zr, and ^{197}Au, give a wide range of A with approximately equal steps in log(A), as is desirable when exponential or power law behaviors are expected. Too, these materials all are available as solid targets with high melting points and high isotopic purities.

3.1 Kinematics

We propose to obtain A dependence data in two kinematic settings, at Q^2 = 1 and 4 $(GeV/c)^2$, and additional Q^2 dependence data on ^{12}C at 2, 3, and 5 $(GeV/c)^2$. We have generally chosen beam energies consistent with 4 or 6 GeV operation of the accelerator and scattering angles that minimize the derived form factor uncertainties for fixed experimental beam time. For all kinematics but the $Q^2 = 4$ $(GeV/c)^2$ point, this gives a figure of merit within about 10% of optimal, and eases potential scheduling conflicts. For the Q^2 = 4 $(GeV/c)^2$ measurement, we request $\approx$ 5.1 GeV beam energy, since this

requires about 30% less beam time than use of a standard beam energy, such as 4.8 or 6.0 GeV, and since we require about a month of beam time for this A dependence measurement.

Optimization considerations include the following. Singles electron count rates for fixed Q^2 are greatest with the highest beam energies, due to the angle dependence of the Mott cross section. However, in measuring coincidences for $(e, e'p)$ with two identical spectrometers, one must also consider kinematic matching. A very forward angle electron leads to a backward angle proton that subtends a much larger solid angle in the laboratory. At lower beam energies, two factors improve the experimental figure of merit. First, the electron and proton can have the same scattering angle and momentum, leading to nearly 100% kinematic matching of the spectrometers. Second, the larger electron angle leads to larger proton polarization, from the $\tan(\theta)$ kinematic factors in the polarization formulae. The interplay between these factors leads to a broad maximum in the figure of merit, centered near the point of best kinematic matching between the spectrometers. Detailed kinematics are given in Table EX.1.

Table EX.1 :

Quasifree kinematics for the proposed measurements.

Quantity	Kin 1	Kin 2	Kin 3	Kin 4	Kin 5
Q^2 $(GeV/c)^2$	1	2	3	4	5
E_e (GeV)	1.6	3.2	4.0	5.06	6.0
θ_e (°)	45.0	31.4	32.5	30.1	28.9
E'_e (GeV)	1.07	2.13	2.40	2.93	3.34
θ_p (°)	41.7	38.9	33.1	30.2	27.7
p_p (GeV)	1.13	1.77	2.36	2.92	3.48
T_p (GeV)	0.533	1.066	1.599	2.132	2.664

3.2 Count Rates

Count rates from a liquid hydrogen target may be simply estimated using the dipole form factor parameterization. These estimates are given in Table EX.2, below. Luminosity for a 10 cm target and a 100 μA beam current would be $2.6\times10^{38}/\mathrm{cm}^2\mathrm{s}$. Detection efficiency is assumed to be 100%. The kinematic matching factor given is the ratio of the solid angle of the proton spectrometer with the solid angle of recoil protons corresponding to electrons in the electron arm. The coincidence rate includes this factor.

Table EX.2 :
Estimated count rates for a hydrogen target and Fermi motion effects for nuclei.

Quantity	Kin 1	Kin 2	Kin 3	Kin 4	Kin 5
kinematic matching (%)	87	67	96	99	92
^{1}H count rate (coinc./s)	8410	1410	367	134	50
θ_{Fermi} (°)	14.8	9.6	7.3	5.9	4.9
% Fermi cone accepted	3.3	7.9	13.9	21.3	30.1
p_{Fermi} accepted (MeV/c,total)	62	96	128	158	188

We anticipate that the lower Q^2 portion of the experiment would run relatively early in Hall A with 100 μA current and 45% polarization. Kin 4 and 5 measurements require beam energies above 4 GeV, and could run separately and much later. For these measurements, we plan to take advantage of anticipated source improvements. We will use the high polarization source to supply 36 μA current at 80% polarization to Hall A, while a second source is supplying beam to the other two halls. While the figure of merit only improves by about 12%, the reduced beam current reduces backgrounds, radiation production in the Hall, and allows the use of thicker targets.

The 3% of a radiation length target is a limit based on calculations that allows no more than about 100 watts of beam power to miss the beam dump.

Of course, the actual operating limit for Hall A will have to be proven during development. The decrease of multiple scattering with beam momentum allows thicker targets at higher energies. Also, with the high polarization source, one can use thicker targets with the reduced beam current to obtain the same beam power missing the dump. The larger polarization would improve the experimental figure of merit almost a factor of 4 for constant luminosity. The limit on luminosity may depend on power deposition at the target. To ensure some safety margin, and to keep radiative corrections from becoming large, we propose to run the higher Q^2 points with targets with twice the thickness, 6 % of a radiation length - this is similar to the total target thickness requested in Hall A experiments with a photon radiator.[52] We plan to investigate the feasibility of using a thicker target.

Our nuclear count rates are estimated relative to the hydrogen rates given above. For a nuclear target, there are four effects that decrease the count rate compared to hydrogen.

1. Fermi motion. Estimates are given in Table EX.2, and this issue is discussed further below.

2. Proton attenuation in the nucleus. Estimates are based on the NE18 data at higher Q^2, and are given in Table EX.3.

3. Decrease in number of protons in the target, at constant areal density. This results from the increasing fraction of neutrons in heavy nuclei. Proton fractions are given in Table EX.3

4. Decrease in areal density, to keep target thickness at 3% of a radiation length - the Hall A design limit. The areal densities of the targets are given in Table EX.3.

Table EX.2 gives an estimate for the size of the Fermi cone, based on the momentum of a free recoiling proton and a Fermi momentum of 0.3 GeV/c.

Assuming that the protons are "uniformly" distributed into a cone of this size, one can make a simple estimate of the effects of Fermi motion on the count rate, also given in Table EX.2. The estimate is the ratio of solid angle subtended by the spectrometer to solid angle subtended by the Fermi cone. The Fermi momentum distribution is not, of course, uniform, but depends on the orbital of the struck nucleon. We have also presented in Table EX.2 an estimate of the region of Fermi momentum with full acceptance for the spectrometer system in each kinematics, based on the horizontal angular acceptance of the spectrometers – this corresponds to perpendicular kinematics. Since we run with the spectrometers about matched, the full Fermi momentum acceptance is about twice the width given in Table EX.2. More precise estimates of Fermi motion effects, using nuclear wave functions within the code MCEEP, are underway.

While for the higher Q^2 point much of the Fermi cone is largely contained within the spectrometer acceptance, we desire at lower Q^2 to measure at a number of angles so that the orbital and recoil momentum dependence of the polarization observables may be mapped out.

The Fermi motion does not make running coincidences on nuclear targets better if one moves the electron either more forward (higher beam energy) or more backward (lower beam energy). In the first case, the 0° protons relative to $\vec{q}$ are more spread out, so the missing momentum acceptance becomes broader, but with a narrower region of full acceptance. Count rates are higher, polarizations are lower, and at the higher Q^2 points less of the acceptance is useful. In the second case, the 0° protons relative to $\vec{q}$ are brought together and only appear in a limited portion of the proton arm acceptance. The full width of the missing momentum acceptance becomes less, and the peak acceptance is increased. count rates decrease, while polarization increases. More spectrometer settings could be needed to cover the full range of the missing momentum acceptance desired.

All of the effects are A dependent, and act to decrease count rates for the heavier targets. Final count rate estimates for the various targets and kinematics are presented in Section 3.5.

Table EX.3 :

Kinematics-independent factors for nuclear count rates.

Target	transmission (%)	protons (%)	areal density* (g/cm^2)	net factor ($f_A/f_{^1H}$)
^1H	1.00	1.00	0.70	1.0
^{12}C	0.63	0.50	1.28	0.58
^{27}Al	0.50	0.48	0.72	0.25
^{56}Fe	0.40	0.50	0.42	0.12
^{90}Zr	0.33	0.44	0.30	0.063
^{197}Au	0.25	0.40	0.20	0.029

* With 3% of a radiation length targets for A > 1.

3.3 Cross Sections

In this experiment, we will measure cross sections and polarizations at the same time. Measurement of absolute cross sections are difficult, in that one must understand the following:

1. Radiative corrections: This is a fairly well-understood theoretical problem. Resulting uncertainties should be of order 1%.

2. Target thicknesses: This experiment uses solid targets, for which the thickness can be determined precisely. Too, all targets proposed have have high melting points and good conductivity, so beam heating effects should be small. Resulting uncertainties should be of order 1%.

3. Beam currents: The precision with which absolute integrated current can be measured should improve at Hall A as a function of time. It

is currently believed that relative current will be available at the 10^{-3} level at turn on from cavity monitors, but absolute current may only be known to several per cent.

4. Spectrometer solid angles and efficiencies: These will probably be determined to no better than a few percent in initial calibrations, but systematics are a concern with any individual method. In this experiment, since we use the same spectrometer settings for all targets, the relative solid angles and efficiencies are of more concern. Since rates are generally low, and the distribution of events across the spectrometer acceptance is roughly A independent, we believe that this relative determination can be checked to be better than 1%.

5. Nuclear wave function corrections: We do not with our spectrometer settings integrate over all possible missing momenta and energies. Thus, we need to use a model for the cross section dependence on these quantities to correct for transmission effects that are merely artifacts of the experimental acceptance. The uncertainties on these corrections will be typically a few per cent.

Since this experiment uses solid targets, and for the $Q^2 = 1$ $(GeV/c)^2$ measurements correspond to proton energies near 500 MeV (see Polarimetry, below), we believe the lower Q^2 part of the experiment is suitable for early running in Hall A if the relative cross sections can be very well determined. Then, if more precise absolute cross sections are needed, these can be determined later by a single absolute measurement on carbon, for which the count rates are high. The main questions for early running in Hall A for the relative cross sections are how well one will actually know the integrated beam current and spectrometer performance. We believe that these quantities will be sufficiently known for very accurate relative measurements.

We propose here a procedure to ensure that the relative cross sections

during the experiment are precisely determined. It is important to note that for these polarization measurements we require typically of order 10^6 counts, and use targets of thickness 3% of a radiation length. Since the spectrometers are designed to give 1 mm resolution (σ) in transverse position at the target, we propose to use a double target at all times, consisting of the target of interest at the pivot point, and a thin ($\approx$ 0.1% of a radiation length, similar to the thickness of the end window on the cryotarget) normalization carbon or aluminum foil located about 2 cm upstream from the pivot. Radiative effects from this thin foil will be minimal. This scheme requires a special target ladder, which we will construct if necessary. The spectrometer angle range in this experiment varies from about 30° to 45°, so the apparent separation of the thin foil form the target is in the range of 10 - 15 σ, for each spectrometer. Because carbon gives the highest count rate, the minimum number of counts we expect to obtain from the thin foil is about 30,000, when it is used with the carbon target at the pivot. Nearly 10^6 counts will be obtained when used with the gold target. This should allow the product of relative luminosity and efficiency to be determined to better than 1%, and will also increase the amount of data collected on carbon by about an order of magnitude, decreasing uncertainties by a factor of three.

3.4 Polarimetry

The focal plane polarimeter is being built by Rutgers and William & Mary, with support from the National Science Foundation. It consists of wire chambers and a large carbon analyzer. The wire chambers are used to track the proton trajectory into and out of the analyzer. Polarized protons scatter from the analyzer with an azimuthal asymmetry, for which the size of the asymmetry is determined by the proton polarization and the analyzing power of the carbon analyzer. Several similar polarimeters at intermediate

energy hadron facilities have been calibrated[53] for kinetic energies up to 800 MeV; these data show that all polarimeters share essentially the same calibration. The POMME polarimeter at Saclay has been calibrated[54] up to 2.4 GeV kinetic energy, and provides the basis for the estimated polarimeter performance in this experiment. The polarimeter analyzing power will be calibrated on site at CEBAF as part of experiment 93-027 (C. F. Perdrisat, V. Punjabi, and M. K. Jones, spokespeople).

The angular distribution of protons scattering from the polarimeter is given by:

$$\frac{d\sigma}{d\Omega}\Big(\theta,\phi\Big) = \frac{d\sigma}{d\Omega_0}\Big(\theta\Big) \times \Big(1 + A_C P'_n \cos(\phi) + A_C P'_t \sin(\phi)\Big). \qquad (23)$$

The interesting range of scattering angle is usually from about 5° to 20°. For these angles, the analyzing power and scattering probability are large, but multiple scattering contributions are small. An angle–averaged analyzing power and integrated probability of scattering in the interesting angle range are given in Table EX.4.

The angular distribution may be Fourier analyzed to determine the transverse and normal components of polarizations in the focal plane. These components are different from the components at the target, due to spin precession effects. In a lowest order view, the proton trajectory bends entirely in a vertical plane due to the horizontal magnetic field of the spectrometer dipole. The transverse spin component, being parallel to the field, is unaffected. The longitudinal and normal spin components rotate into each other. Thus, the normal component of polarization in the focal plane is given by:

$$P'_n = \cos(\chi)P_n + \sin(\chi)P_l, \qquad (24)$$

where the spin precession angle χ is given by:

$$\chi = (\frac{g-2}{2})\omega\gamma. \qquad (25)$$

Here $\omega = 45°$ is the bend angle of the spectrometer for central rays, $\gamma = E/M_p$ is the usual Lorentz factor, and the numerical value of $(g-2)/2$ is 1.79. Spin precession angles are also given in Table EX.4.

Spin transport uncertainties are worst at the $Q^2 = 5$ kinematics, since the spin precession is closest to rotating the longitudinal component back to longitudinal for this energy proton. We can estimate the change in calculated P_l for small changes in spin precession χ as

$$\Delta(P_l)/P_l = -\Delta(\chi)\cot(\chi). \tag{26}$$

Percentage uncertainties in spin precession resulting from a 1 mr systematic uncertainty in angle determination - ultimate angular determination should be about 0.5 mr - are given in Table EX.4. Uncertainties during early running may be several mr in angle, leading to systematic uncertainties on the form factor ratios of perhaps 1%. This expected systematic uncertainty is small compared to the expected 10% statistical uncertainty.

The uncertainty in the polarizations determined by the Fourier analysis is given by:

$$\Delta P = \frac{\pi}{2A_C h\sqrt{\epsilon N}}. \tag{27}$$

Here the beam helicity h has been explicitly included, since we are actually interested in the polarization transfer coefficients, which are equivalent to the polarizations obtained if the beam helicity is 1. The factor ϵ is the polarimeter efficiency. Since the same uncertainty applies to both components of the polarization, we can express the relative uncertainty on the form factor ratio $R_G = G_E/G_M$ as:

$$\frac{\Delta R_G}{R_G} = \Delta P\sqrt{\frac{1}{P_t^2} + \frac{1}{\sin^2(\chi)P_l^2}}. \tag{28}$$

The uncertainty on the form factor ratio, $R_F = F_2/F_1$, is found by differentiating the expression relating the ratios R_G and R_F from Section 2.1. We

obtain:

$$\frac{\Delta R_F}{R_F} = \frac{\Delta R_G}{R_G} \times \left(\frac{-R_G(1+\tau)}{(\tau + R_G)(1 - R_G)}\right). \quad (29)$$

The percentage uncertainties on R_F are about equal to and 70% as large as those on R_G for the A dependence data at $Q^2 = 1$ and 4 $(GeV/c)^2$, respectively.

Polarization observables can be estimated for the proton by using the dipole form factor parameterizations. These estimates are in Table EX.4. For nuclear targets, it is expected that *polarization transfer observables are approximately equal to those for the free proton, for all orbitals, as long as the recoil momentum is somewhat smaller than the Fermi momentum*, less than about 200 MeV/c. We will experimentally check the validity of this statement on the nuclear targets at the lower Q^2 point, for which beam time requirements are much smaller.

The polarization components are given for a beam polarization of 100%. The actual beam helicity, expected to be 45%, does not affect the ratio of longitudinal to transverse components, but does change the uncertainties, as indicated above. The normal component of the polarization is 0 for a proton target, but is nonzero and dependent on the orbital and the Fermi momentum for nuclear targets. The orbital dependence of P_n does not affect our proposed measurement, since the distribution of events among various orbits is unchanged when the beam helicity is reversed.

Thus, one separates out the components by reversing the spin of the beam, which reverses the direction of P_l and P_t, but not of P_n. One then extracts P_l from the difference in measured normal spin at the focal plane with the beam helicity reversed. *Determining P_l and P_t by reversing the beam helicity removes any focal plane polarimeter false asymmetries and any normal polarization component at the target.* There are still systematic uncertainties associated with the beam polarization flip and the recoil proton spin transport, both of which are expected to be small. The data for P_n are

not the focus of this experiment, but as P_n arises from rescattering of the outgoing proton, these data will be available for analysis and should provide a check on the extracted attenuation cross section.

Table EX.4 :

Polarization observables for a proton target, for h = 1.

Quantity	Kin 1	Kin 2	Kin 3	Kin 4	Kin 5
Polarimeter efficiency (%)	16	20	33	44	47
Polarimeter A_C	0.33	0.20	0.13	0.10	0.10
P_l	0.548	0.507	0.581	0.546	0.613
P_t	-.333	-.227	-.210	-.186	-.171
P_n	0.000	0.000	0.000	0.000	0.000
spin precession χ (°)	227	309	391	473	555
P'_n	-.399	-.394	0.300	0.502	-.163
$\Delta P'_n/\Delta\chi$ (%/mr)	0.093	-0.065	0.166	-0.042	0.373

3.5 Beam Time Request and Schedule

Estimated count rates, total times, and expected uncertainties for the ratios of form factors G_E/G_M and F_2/F_1 are given in Tables EX.5 and EX.6 for the measurements of A dependence, and in Table EX.7 for the measurements of Q^2 dependence on ^{12}C. At $Q^2 = 1$ (GeV/c)^2, 1.1×10^6 counts lead to an uncertainty on the polarization components of ±0.025, and uncertainties of about 10% on the ratios F_2/F_1 and G_E/G_M. At $Q^2 = 4$ (GeV/c)^2, due to the lower analyzing power of the polarimeter, but the higher polarization assumed for the beam, 1.5×10^6 counts lead to an uncertainty on the polarization components of ±0.024, and uncertainties of about 10% on the ratio F_2/F_1 and 14% on the ratio G_E/G_M.

For the nuclear targets at $Q^2 = 1$ (5) (MeV/c)^2, the spectrometer acceptance corresponds to a total acceptance in Fermi momentum for perpendicular kinematics of about 60 (190) MeV/c. This is the region with full

acceptance; the tails of the acceptance span a region about twice as large. At $Q^2 = 1$ (GeV/c)^2, we will measure at least two recoil proton angles on each target so that the polarization may be mapped out over the region of missing momentum from 0 to 200 MeV/C. For the ^{12}C target, we will take four kinematic settings and run each for twice as long, so that the recoil momentum acceptance may be binned finer and studied over a wider range.

Table EX.5 :

Count rates and times at $Q^2 = 1$ (GeV/c)^2. In all cases, expected uncertainties are ± 0.025 for the measured polarization, leading to an uncertainty of $\pm 9.8\%$ for the ratio of G_E/G_M, and of $\pm 10.0\%$ for the ratio of F_2/F_1, at each angle setting.

Target	Data rate (Hz)	Time (Hrs)	Number of Angles	Total beam time (Hrs)
^{1}H	8410.0	0.04	0	0*
^{12}C	105.0	3.0	8	24
^{27}Al	45.0	7.	2	14
^{56}Fe	22.4	14.	2	28
^{90}Zr	11.4	26.	2	52
^{197}Au	5.2	59.	2	118
Total				236
Overhead				28

* ^{1}H count rates are presented for comparison only; we do not propose to measure ^{1}H.

For the A dependence at $Q^2 = 4$ (GeV/c)^2, only a single kinematic setting is needed because of the missing momentum acceptance of the spectrometers, a 160 MeV/c range of missing momentum with full acceptance, and a 320 MeV/c range over which there is some acceptance. The decrease in count rates from the drop in the form factors with Q^2 makes 10% measurements for all targets very expensive in beam time. Our time estimates and the

resulting uncertainties are shown in Table EX.6. As a result, we relax the statistical requirements somewhat for the heavier targets.

Table EX.6 :

Count rates and times for $Q^2 = 4$ (GeV/c)^2 kinematics. For the heavier targets, statistics are reduced and uncertainties are increased as indicated.

Target	Data rate (Hz)	Time (Hrs)	Uncertainty P (%)	Uncertainty G_E/G_M (%)	Uncertainty F_2/F_1 (%)
^{1}H	48.3	9.4*	2.4	14.	10.
^{12}C	7.86	58	2.4	14.	10.
^{27}Al	3.41	133	2.4	14.	10.
^{56}Fe	1.64	123	3.6	20.	15.
^{90}Zr	0.86	133	4.8	28.	20.
^{197}Au	0.40	284	4.8	28.	20.
Total		731			
Overhead		28			

* ^{1}H count rates are presented for comparison only; we do not propose to measure ^{1}H.

Rates and times for the study of the Q^2 evolution of the form factors on ^{12}C are given in Table EX.7. Times include two kinematic settings for $Q^2 =$ 2 and 3 (GeV/c)^2, to provide coverage of a range of Fermi momenta. Rates are for a 6 % of a radiation length target for Kin 4 and 5.

Table EX.7 :

Summary of count rates and times for ^{12}C at all Q^2. The Kin 1 and Kin 4 settings are part of the A dependence measurements, times ar in Tables EX.5 and EX.6. Statistical precision is 10% for the ratio F_2/F_1, except for an increase to 15% for Kin 5.

Quantity	Kin 1	Kin 2	Kin 3	Kin 4	Kin 5
Q^2 (GeV/c)^2	1	2	3	4	5
^{12}C rate (Hz)	105	42	20	7.9	4.2
Time (hours)	-	38	122	-	84
Overhead time (hours)	-	9	9	-	8

We plan to run the experiment in two stages. The first stage will encompass all data points requiring 4 GeV beam energy or less, and include Q^2 = 1, 2, and 3 $(GeV/c)^2$ points. Our beam time request is for 10.0 days of beam at 1.6 GeV, 1.5 days of beam at 3.2 GeV, and 5.0 days of beam at 4.0 GeV, for a total of 16.5 days. We estimate overhead to be 24 hours for initial setup of targets and equipment, 8 hours for each of the two beam energy / spectrometer momentum changes, and about 1 hour for each of the 28 data points to select target and set spectrometer angles, and to check beam polarization. This leads to a request for 3 days of overhead time. We emphasize that this portion of the measurement is very appropriate for early running at CEBAF Hall A.

In the second phase of the experiment, we will obtain the data for beam energies greater than 4 GeV, corresponding to the Q^2 = 4 and 5 $(GeV/c)^2$ points. We request 30.5 days of beam at 5.06 GeV, and 3.5 days of beam at 6.0 GeV, for a total of 34 days. Estimated overhead is 24 hours for initial setup of targets and equipment, 8 hours for the beam energy / spectrometer momentum change, and about 1 hour for each of the 6 data points. A few additional hours might be needed for extra beam polarization checks. This leads to a request for 1.5 days of overhead time.

Appendix I

Individuals participating in this collaboration:

A. Afanasev, F. T. Baker, L. Bimbot, E. J. Brash, W. Bertozzi,

J. Calarco, J. P. Chen, D. Dale, J. E. Ducret, J. M. Finn,

V. Ganenko, A. Gasparian, S. Gilad, R. Gilman, A. Glamazdin,

C. Glashausser, V. Gorbenko, C. Howell, M. Jones, G. Kumbartzki,

R. Michaels, S. Nanda, C. F. Perdrisat, V. Punjabi, R. Ransome,

P. M. Rutt, A. Saha, A. Sarty, P. Sorokin, P. E. Ulmer,

A. Voskanian, L. Weinstein, J.-C. Yang

References

[1] N. C. R. Makins *et al.*, Phys. Rev. Lett. **72**, 1986 (1994).

[2] T. G. O'Neill *et al.*, unpublished preprint HEP-PH-9408260 (1994).

[3] J. Nemchik, N. N. Nikolaev, and B. G. Zakharov, Workshop on CEBAF at Higher Energies, 415 (1994).

[4] L. L. Frankfurt, M. M. Sargsyan, M. I. Strikman, Workshop on CEBAF at Higher Energies, 499 (1994).

[5] D. F. Geesaman *et al.*, Phys. Rev. Lett. **63**, 734 (1989).

[6] G. Garino *et al.*, Phys. Rev. **C45**, 780 (1992).

[7] V. R. Pandharipandhe and S. C. Pieper, Phys. Rev. **C45**, 791 (1992).

[8] G. van der Steenhoven *et al.*, Phys. Rev. Lett. **57**, 182 (1986); **58**, 1727 (1987).

[9] P. E. Ulmer *et al.*, Phys. Rev. Lett. **59**, 2259 (1987).

[10] D. Reffay-Pikeroen *et al.*, Phys. Rev. Lett. **60**, 776 (1988).

[11] A. Magnon *et al.*, Phys. Lett. **222B**, 1276 (1989).

[12] CEBAF proposal exp. 93-049, J. F. J. van den Brand, Rolf Ent, and P. E. Ulmer, spokespeople, unpublished (1993).

[13] T. D. Cohen, J. W. van Order, and A. Pickleshimer, Phys. Rev. Lett. **59**, 1267 (1987).

[14] T. Suzuki, Phys. Rev. **C37**, 549 (1988).

[15] M. Kohno, Phys. Rev. **C38**, 584 (1988).

[16] J. V. Noble, Phys. Rev. Lett. **46**, 412 (1981).

[17] C. E. Carlson and T. J. Haven, Phys. Rev. Lett. **51**, 261 (1983).

[18] L. S. Calenza, A. Rosenthal, and C. M. Shakin, Phys. Rev. Lett. **53**, 892 (1984); L. S. Calenza, A. Rosenthal, and C. M. Shakin, Phys. Rev. **C31**, 232 (1985).

[19] P. J. Mulders, Phys. Rev. Lett. **54**, 2560 (1985).

[20] E. M. Henley and G. Krein, Phys. Lett. **B231**, 213 (1989).

[21] S. Krewald, Phys. Lett. **222B**, 338 (1989).

[22] Pankaj Jain and John P. Ralston, Phys. Rev. **D48**, 1104 (1993). See also John P. Ralston in *Perspectives in Hadronic Structure*, NATO Advanced Study Institute, Drouten, Netherlands (1993), ed: Mittarakeh *et al.*

[23] John P. Ralston, private communication.

[24] G. Peter LePage and Stanley J. Brodsky, Phys. Rev. **D22**, 2157 (1980).

[25] P. Bosted *et al.*, Phys. Rev. Lett. **68**, 3841 (1992).

[26] Felix Schlumpf, unpublished, available as SLAC publication 6502, or preprint HEP-PH-9408260 (1994).

[27] P. Kroll, unpublished, available as Wuppertal publication WU-B 94-17 or preprint HEP-PH-9409262 (1994).

[28] Pankaj Jain, John P. Ralston, and Bernard Pire, *High Energy Hadronic Helicity Violation: What Helicity Flip Form Factors Measure*, Proceedings Division Particles and Fields, American Physical Society, (Fermilab 1992).

[29] Pankaj Jain and John P. Ralston, *Measuring Chirally Odd Wave Functions with Helicity Flip Form Factors*, Future Directions in Particle and Nuclear Physics at Multi-GeV Hadron Beam Facilities, 4–6 March 1993, Brookhaven National Laboratory Report BNL-52389, pg. 217.

[30] **Polarization Transfer in the ^{3}He$(\vec{e}, e'\vec{p})$d and ^{3}He$(\vec{e}, e'\vec{p})$pn Reactions**, submitted to PAC 9 (R. Ransome, contact person, E. J. Brash, P. M. Rutt, and S. Nanda, spokespeople).

[31] M. N. Rosenbluth, Phys. Rev. **79**, 615 (1950).

[32] D. R. Yennie, M. M. Levy, and D. G. Ravenhall, Rev. Mod. Phys. **29**, 144 (1957).

[33] N. Dombey, Rev. Mod. Phys. **41**, 236 (1969).

[34] A. I. Akhiezer and M. P. Rekalo, Fiz. El. Chast. Atom. Yad. **4**, 662 (1973) [Sov. J. Part. Nucl. **4**, 277 (1974)].

[35] Raymond G. Arnold, Carl E. Carlson, and Franz Gross Phys. Rev. **C23**, 363 (1981).

[36] R. G. Arnold *et al.*, Phys. Rev. Lett. **57**, 174 (1986).

[37] A. F. Sill *et al.*, Phys. Rev. **D48**, 29 (1993).

[38] G. Farrar, private communication.

[39] T. de Forest Jr., Nucl. Phys. **A392**, 232 (1983).

[40] X. Song, J. P. Chen, P. K. Kabir, and J. S. McCarthy, J. Phys. G **17**, L75 (1991).

[41] X. Song, J. P. Chen, and J. S. McCarthy, Z. Phys. A **341**, 275 (1992).

[42] R. Schiavella, private communication.

[43] A. Afanasev, private communication.

[44] See MIT Bates proposal 88-21 (J. M. Finn, R. W. Lourie, C. F. Perdrisat, and P. E. Ulmer, spokespeople).

[45] See CEBAF proposal 93-049 (J. F. J. van den Brand, Rolf Ent, and P. E. Ulmer, spokespeople).

[46] D. G. Ireland, L. Lapikas, and G. van der Steenhoven, Phys. Rev. **C50**, 1626 (1994).

[47] Richard A. Arndt, L. David Roper, Ron L. Workman, and M. W. McNaughton, Phys. Rev. **D45**, 3995 (1992).

[48] A. Mueller, *Proceedings of the Seventeenth Recontre de Moriond on Elementary Particle Physics*, (Les Arcs, France 1982) edited by J. Tran Thanh Van (Editions Frontieres, Gif-sur-Yvette, France 1982), p. 13; S. J. Brodsky, in *Proceedings of the Thirteenth International Symposium on Multiparticle Dynamics*, edited by W. Kittel, W. Metzger, and A. Stergiou (World Scientific, Singapore, 1982) p. 963.

[49] L. Frankfurt, G.A. Miller, M. Strikman, Comments Nucl. Part. Phys. **21**, 1 (1992) and references therein.

[50] A.S. Carroll *et al.* Phys. Rev. Lett. **61**, 1698 (1988).

[51] J.P. Ralston and B. Pire, Phys. Rev. Lett. **65**, 2343 (90).

[52] CEBAF experiments 89-019 (R. Gilman, R. J. Holt, Z.-E. Meziani, spokespeople) and 94-012 (R. Gilman and R. J. Holt okespeople).

[53] M. W. McNaughton *et al.*, Nucl. Inst. Meth. **A241**, (1985).

[54] V. Punjabi *et al.*, Bull. Am. Phys. Soc. **38**, 1036 (19 ; V. Punjabi *et al.*, Bull. Am. Phys. Soc. **36**, 1302 (1991); and B. B in *et al.*, Nucl. Inst. Meth. **A288**, 389 (1990).